

Polystyrene Network–Network Interdiffusion

U. Perez-Salas

Chemical Physics Program, University of Maryland, College Park, Maryland 20472

R. M. Briber*

Department of Materials and Nuclear Engineering, University of Maryland, College Park, Maryland 20472

W. A. Hamilton

Neutron Scattering Group, Building 7962, Mail Stop 6393, Oak Ridge National Laboratory, Oak Ridge, Tennessee 37831-6393

M. H. Rafailovich and J. Sokolov

Department of Materials Science and Engineering, SUNY, Stony Brook, New York 11794

L. Nasser

Institute for Physical Science and Technology, University of Maryland, College Park, Maryland 20472

Received May 14, 2001; Revised Manuscript Received April 15, 2002

ABSTRACT: Neutron reflectivity was used to study the interdiffusion of thin film bilayers of cross-linked deuterated and protonated polystyrene. The films were spun-cast and cross-linked by γ radiation. Interfacial broadening was studied as a function of annealing time for different cross-link densities. The samples were annealed in a vacuum at 150 °C, and neutron reflectivity measurements were performed in air at room temperature. The interface was observed to broaden rapidly at short annealing times and then plateau to an equilibrium value. The interfacial broadening was modeled using a solution to the Fokker–Planck equation with a parabolic external potential to obtain the equilibrium interfacial width and effective diffusion coefficient as a function of the average network mesh size, \bar{N}_c . The interfacial width was found to scale as $\bar{N}_c^{0.47 \pm 0.1}$. The effective diffusion coefficient was found to be independent of \bar{N}_c .

Introduction

The diffusion of polymer molecules as a function of chain architecture is an important factor in determining many practical processes such as adhesion, interface formation, and phase separation. Previous research has centered in understanding mutual diffusion in polymer melts and its dependence on molecular weight.^{1,2} More recently, there has been work on the diffusion of linear homopolymers into their homologous cross-linked state. This work focused in obtaining the diffusion coefficient, D , as a function of \bar{N} , the average degree of polymerization of the diffusing chain, and \bar{N}_c , the average number of repeat units between cross-links in the network.^{3–5} The studies generally agree with the reptation model as proposed by de Gennes which describes the mobility of isolated chains in a network and predicts the diffusion coefficient, D , as inversely proportional to the square of \bar{N} ($D \sim \bar{N}^{-2}$).⁶ In general, the scaling exponent of -2 in reptation is valid in the regime where the length of the linear chains (\bar{N}) diffusing into the network and the mesh size of the network (\bar{N}_c) are larger than the characteristic entanglement length (\bar{N}_e). In addition, for large values of the \bar{N}/\bar{N}_c ratio, diffusion essentially stops due to limited solubility of the linear chains in the network.^{7,8}

The expectation of cutoff in D for a given \bar{N}_c below which diffusion should slow dramatically and/or stop for a given length of the linear chains, \bar{N} , is consistent with

the free energy describing the swelling of networks by linear chains, given by^{7,9}

$$\frac{\Delta f}{kT} = \frac{3A}{v_c \bar{N}_c} (\phi_s^{2/3} \phi^{1/3} - \phi) + \frac{B\phi}{v_c \bar{N}_c} \ln(\phi/\phi_s) + \frac{(1 - \phi) \ln(1 - \phi)}{v \bar{N}} + \frac{\chi}{v_0} \phi(1 - \phi) \quad (1)$$

Equation 1 is composed of an elastic term and a mixing term which compete and give rise to phase separation for particular sets of \bar{N}_c and \bar{N} . In eq 1, v and v_c are the molar volumes of the linear chain monomer unit (solvent) and the network monomer unit (v and v_c being the same in homologous systems), v_0 is the reference unit volume ($v_0 = \sqrt{vv_c}$), χ is the Flory interaction parameter, ϕ is the volume fraction of the network in the swollen state, ϕ_s is the reference state of the network, usually taken as the volume fraction of network when it was formed, and A and B are constants. Generally, these are taken to be $A = 1/2$ and $B = 1/f$ by Flory, where f is the functionality of the cross-link points.⁹

Network–network interdiffusion of homologous materials has been studied by Geoghegan et al., using neutron reflectivity.¹⁰ The network bilayers were formed from chemically cross-linked protonated and deuterated polystyrene films. They found that the interface reached an equilibrium width after short annealing times. It is reasonable to expect that the interfacial width between

* To whom correspondence should be addressed.

cross-linked networks should increase at short annealing times and then reach a plateau at a relatively narrow width due to the presence of the cross-links. A polymer network is an elastic solid, and because two networks cannot interdiffuse on a macroscopic scale, they can be considered immiscible. Local rearrangements at the interface can still be expected to occur due to the mobility of the network chains between cross-links and interpenetration of dangling ends, which are driven by the local free energy. The value of the equilibrium width attained by the system should depend on the mesh size of the networks with a power law given by $w_{\text{eq}} \sim \bar{N}_c^\alpha$, where α is a scaling exponent. In the vicinity of the gel point, it is likely that this behavior would change as long-range diffusion can start to occur. However, Geoghegan et al. did not attempt to extract a value for α because the equilibrium widths they obtained did not have a clear \bar{N}_c^α dependence. Only for their tighter network did they find a narrower equilibrium width than for the less cross-linked samples. Their inability to distinguish different equilibrium widths as a function of \bar{N}_c is probably due to the fact that their films were thick (3500 Å), and thus small interdiffusion changes become smeared out due to instrumental resolution.

This paper will discuss measurements of network–network interdiffusion by neutron reflectivity. The system studied consists of radiation cross-linked protonated and deuterated polystyrene bilayers, each film of approximately 500 Å. Two types of bilayers were prepared. One type consisted of bilayers formed with independently cross-linked films. The second type consisted of bilayers formed with un-cross-linked films which then were cross-linked as a unit. The experiments will focus on obtaining the interfacial width of the bilayers as a function of annealing time and the dependence of this equilibrium width on the mesh size of the network. The kinetics of interface interdiffusion will be examined using a model based on the solution of the Fokker–Planck equation for Brownian motion with a parabolic potential.¹¹

Experimental Section

Solutions in toluene of narrow molecular weight distribution of anionically polymerized protonated polystyrene (HPS) and deuterated polystyrene (DPS) with molecular weights 727.5 and 698 kg/mol ($M_w/M_n = 1.08$ and 1.05), respectively, obtained from Polymer Source, Inc., were spun-cast onto glass to form thin films and floated off on deionized water. The films were picked up from underneath on a piece of glass covered with Al foil using a mechanical lever system to raise the substrate slowly enough so that the water at the film–substrate interface had time to drain. The Al foil coated with the polymer films was separated from the glass and placed in a Pyrex tube, which was then evacuated and sealed. The vacuum system connected to the glass manifold consisted of a rotary pump and a diffusion pump with a liquid N₂ trap system. The pressure attained was 2×10^{-6} Torr, measured by an ion gauge located prior to the connection to the manifold. The tubes were evacuated for 24 h and maintained at 72 °C using an oil bath. To cross-link the samples, the Pyrex tubes were placed inside a Co-60 γ cell that was kept at room temperature through a water cooling system.^{12–14} Once irradiated, the Al foil was dissolved in a 1% HCl solution using deionized water. The films were cleaned by diluting the residual acid solution many times with deionized water. The films were then picked up on Si wafers using the method described above. The native oxide layer of the Si wafer was removed with buffered HF (1 min exposure) prior to picking up a film. The bilayers were formed with one HPS and one DPS thin film since neutron reflection

relies on deuteration for contrast. Two types of cross-linked bilayer samples were made. The first type consisted of two films that were cross-linked independently and then brought together, so that the bilayers were formed after the cross-linking process. These samples were designated as independent or “i”. The second type consisted of bilayers formed with two un-cross-linked films, and then the bilayer was cross-linked as a single unit. These were samples designated as together or “t”. It is expected that the bilayers formed before the cross-linking process will have some cross-links existing between the layers (i.e., between the H and D chains). One of the goals of this work is to compare the behavior of these two types of systems. The deuterated film was always the one in contact with the Si wafer in the neutron reflection experiments to allow for better contrast at the polymer–Si interface. The thickness of the films was determined using ellipsometry, and the quality of the films was also checked using X-ray reflectivity prior to the neutron reflectivity experiments. \bar{N}_c values for all the networks used were calculated on the basis of swelling measurements in toluene of reference polystyrene pellets that were cross-linked at the same time as the films (the pellets were formed with polystyrene homopolymer $M_w = 970\,000$ g/mol, $M_w/M_n = 1.41$ obtained from Polymer Source, Inc.).

The \bar{N}_c values were calculated using the following equation:^{7,9}

$$\bar{N}_c = \left(\frac{\phi}{2v_c} - \frac{\phi^{1/3}}{v_c} \right) \left(\frac{\phi + \ln(1 - \phi)}{v} + \frac{\chi}{v_0} \phi^2 \right)^{-1} \quad (2)$$

This equation is obtained by evaluating the chemical potential of the solvent molecules, $\partial(n_T \Delta f / kT) / \partial n$ (Δf is given by eq 1, n_T is the total number of moles in the system, and n is the number of moles of solvent in the system), and equating it to zero, as the swollen network is assumed to be in equilibrium with a phase of pure solvent. For the swelling measurements ϕ_s was set equal to 1, f , the functionality of the cross-link points, equal to 4, and $\chi_{\text{PS/toluene}} = 0.44$.¹⁵

Previous work by Patel et al. has shown that eq 2 for both model and imperfect networks is incorrect by a prefactor.¹⁶ Also, they found that each type of network has its own prefactor. This means that eq 2 should really be written as

$$\kappa \bar{N}_c = \left(\frac{\phi}{2v_c} - \frac{\phi^{1/3}}{v_c} \right) \left(\frac{\phi + \ln(1 - \phi)}{v} + \frac{\chi}{v_0} \phi^2 \right)^{-1} \quad (3)$$

where κ is the prefactor for a given type of network. The prefactor corrects for the difference between the actual experimentally measured modulus, which includes the effect of trapped entanglements, and the theoretical modulus, which ignores entanglement effects. However, because the focus of this work is to find general scaling trends, this prefactor does not affect the exponent for \bar{N}_c , and eq 2 can be used accordingly.

The \bar{N}_c values obtained with eq 2 were 140 ± 5 , 230 ± 5 , 480 ± 10 , 680 ± 30 , 1310 ± 10 , 1510 ± 30 , and 1700 ± 110 . Each \bar{N}_c value is the average of several measurements on the same pellet, and the reported error is the standard deviation. To estimate systematic errors, measurements on different pellets of equivalent cross-link density were performed for some of the cross-link densities studied, and no significant difference was found in the values of \bar{N}_c . At the gel point, defined as one cross-link unit per weight-average molecule, \bar{N}_c is approximately 7000. All films were approximately 450 Å thick, except the films with $\bar{N}_c = 1700$, whose thickness was approximately 700 Å due to an initial slightly more concentrated polymer solution.

Neutron reflectivity measurements were all done at room temperature in air. The annealing prior to measuring was done in a vacuum oven at 150 °C. The annealing times were 0, 5, 30, 60, 180, 480, and 1140 min. Neutron reflectivity measurements were obtained using the NG7 horizontal stage reflectometer at the Center for Neutron Research at the National Institute of Standards and Technology in Gaithersburg, MD,

and the reflectometer in the High Isotope Flux Reactor at Oak Ridge National Laboratory.^{17–19} The range of momentum transfer, q ($q = (4\pi/\lambda) \sin \theta$, where θ is the incident angle of the neutron beam), was $0.005 < q < 0.16 \text{ \AA}^{-1}$. The data were analyzed using the nonlinear least-squares fitting routine found within the program for reflectivity instrument control, data collection, data reduction and analysis named "Mirror".²⁰

Results and Discussion

Analysis of the reflectivity data was performed by postulating a stepped scattering length density profile with a hyperbolic tangent function and/or an error function describing the interfaces. The reflectivity was calculated by iterative reflectance calculations at the interfaces of the steps, and the parameters were adjusted by a nonlinear least-squares fitting routine to minimize χ^2 defined as $\chi^2 = \sum_i (F_i - f_i)/\epsilon_i^2$ where F_i is the value of the i th data point with ϵ_i its statistical error and f_i its value obtained from the fit.^{20,21} The scattering length density profile, $\rho(z)$, describing the interface between the films was based on a Fickian-type diffusion profile:²²

$$\rho(z)_{z \geq 0} = A \left(-\operatorname{erf}\left(\frac{z - \delta}{\omega}\right) + \operatorname{erf}\left(\frac{z + \delta}{\omega}\right) \right) \quad (4)$$

where A is a constant, δ is the film thickness, and ω , the interfacial width, is $\sqrt{2}$ times the half-width at half-maximum of the derivative of eq 4 which is a Gaussian.

The scattering length density profile was modified from eq 4 to include a discontinuity at the interface between the films. The discontinuity reflects the relation between diffusion in network–network interfaces and diffusion in symmetric linear polymer interfaces for times t shorter than the reptation time T_{rep} . In symmetric linear polymer interfaces, for $t < T_{\text{rep}}$, all interdigitation is due to chain ends. Because the chain ends are originally reflected away from the interface, most tube motions in this time interval do not lead to intertwining, and this results in a discontinuous scattering length density profile. The discontinuity persists up to interfacial widths close to the radius of gyration of the chains, when $t \approx T_{\text{rep}}$.^{23–25} Cross-linking fixes the original chains, which means that the only tube motion is that of the dangling ends of the network (the chain ends of the original polymer). The cross-links, however, now restrict the motions of the dangling ends to a width on the order of the coil size of the dangling ends, which is less than the coil size of the original chain, and therefore the profile can always remain discontinuous. From a macroscopic point of view, the discontinuity is physically reasonable because networks are soft solids that allow some interpenetration, but not enough to make the interface completely disappear. The discontinuity at the interface generates a calculated reflectivity curve that continues to oscillate at high q , in contrast to a scattering length density profile with no discontinuity where the peaks at high q are damped.²⁶ Figure 1a shows example reflectivity data as a function of q and corresponding calculated reflectivity (plotted as continuous curves) for a bilayer with $\bar{N}_c = 140$ formed after the films were independently cross-linked and for a bilayer with $\bar{N}_c = 1510$ that was formed before being cross-linked. Figure 1b,c shows the corresponding scattering length density profiles. The annealing times shown are 0 and 180 min. The samples are labeled 140_i and 1510_t, where "i" stands for a bilayer formed with films cross-linked independently and where "t" stands

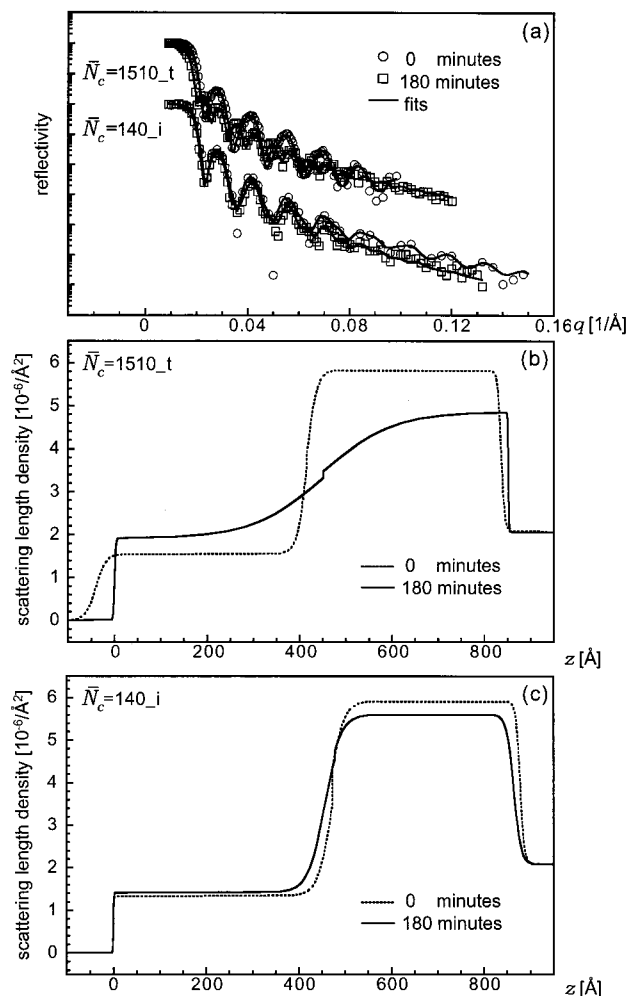


Figure 1. (a) Reflectivity data for a bilayer with $\bar{N}_c = 140$ formed after the films were independently cross-linked ($\bar{N}_c = 140_i$, "i" stands for "independent") and for a bilayer with $\bar{N}_c = 1510$ that was formed with un-cross-linked films and then cross-linked as a unit ($\bar{N}_c = 1510_t$, "t" stands for "together") for 0 and 180 min annealing at 150°C . The solid lines through the data correspond to the fits resulting from the scattering length profiles shown in (b) and (c). Each film was approximately 450 \AA .

for un-cross-linked films forming a bilayer which are then cross-linked together as a unit. From Figure 1b,c it can be seen that although the interfaces became smoother after long annealing times, the discontinuity does not fully disappear. The fits correlated well with the ellipsometry thickness measurements made on single films and on bilayers. Sol molecules are created in the irradiation process, and during annealing the layers exchange sol molecules (which on the average are smaller than \bar{N}_c). This exchange lowers the average scattering length density of the DPS layer and increases the average scattering length density of the HPS layer, as shown in Figure 1b,c. The sample with $\bar{N}_c = 1700$, which is the sample closest to the gel point value (i.e., the loosest network), had a qualitatively different scattering length density profile for long annealing times. At this cross-link density the sol fraction is sufficient to show a significantly reduced diffusion rate near the Si wall.²⁷ Figure 2a shows the scattering length density profile for the sample with $\bar{N}_c = 1700$ annealed for 0 and 1140 min at 150°C .

The interfacial width between the networks rapidly plateaus to an equilibrium value as a function of

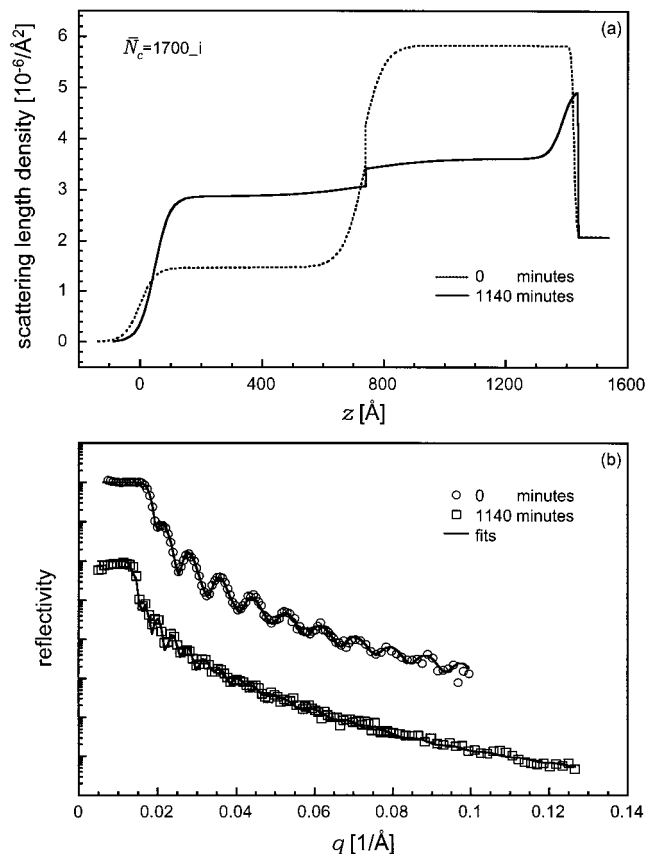


Figure 2. (a) Scattering length density profiles for the bilayer with $\bar{N}_c = 1700$ formed after the films were independently cross-linked and annealed for 0 and 1140 min at 150 °C. Each film was approximately 700 Å. (b) Reflectivity data and fits (the continuous curves through the data) obtained from the scattering length density profiles in (a).

annealing time. Figure 3 shows the interfacial widths as a function of annealing time for two samples with $\bar{N}_c = 1510$ and one sample with $\bar{N}_c = 140$. In principle, it is possible to obtain the diffusion constant from the time dependence of the interfacial width (ω in eq 4). To establish the kinetics of the interfacial width, one can model the interface as a collection of particles undergoing Brownian motion subject to an external force field. The interdiffusion behavior of the two networks is expected to obey Brownian-type motion as the two networks are identical except for deuterium labeling. There is a thermodynamic factor due to the small H/D Flory χ parameter, but it is expected to play a secondary role compared to the elasticity of the networks resisting long-range interdiffusion. The small Flory χ parameter can be important in high molecular weight linear blend systems, where there is no elastic energy term in the free energy. However, in cross-linked blend systems, the elastic contribution to the free energy generally dominates.⁷ In general, Brownian-type systems can be described by the Fokker–Planck equation:¹¹

$$\frac{\partial P(z,t)}{\partial t} = \left[\frac{1}{\gamma} \frac{\partial}{\partial z} \left(\frac{dV(z)}{dz} \right) + D \frac{\partial^2}{\partial z^2} \right] P(z,t) \quad (5)$$

where $P(z,t)$ is the probability distribution, D is the effective diffusion constant, γ is the friction coefficient, and $V(z)$ is the external potential. When the external field is constant, eq 5 reduces to Fick's second law. $P(z,t)$, properly renormalized, can represent the scattering

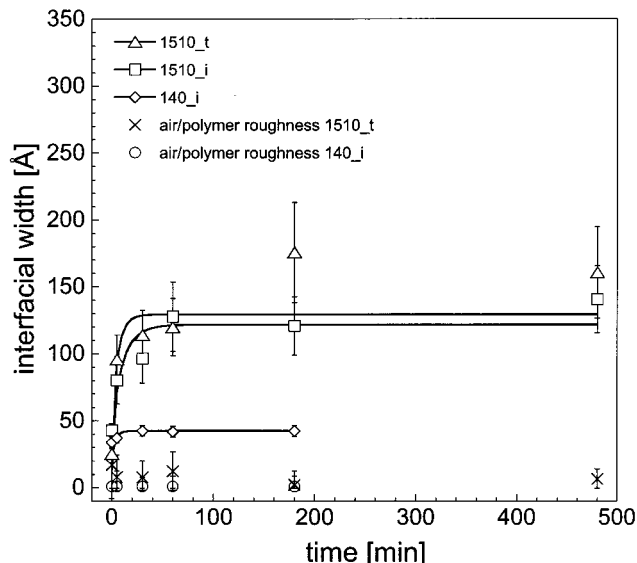


Figure 3. Interfacial widths for samples with $\bar{N}_c = 1510$ and $\bar{N}_c = 140$ as a function of time. The solid lines represent the fits to the widths using eq 9 with $t \rightarrow t + t_0$. The roughness of the polymer–air interface for the samples is included for comparison.

length density profile at a time t . Taking the limit $t \rightarrow \infty$ in eq 5, we can solve for the potential explicitly:

$$V(z) = -\gamma D \ln P(z, t \rightarrow \infty) \quad (6)$$

where $P(z, t \rightarrow \infty)$ is now the scattering length density profile at long annealing time when the system has reached its equilibrium state. The complicated form of the potential makes the extraction of an exact analytical solution intractable. However, one can expand the potential in powers of $z' = z - \delta$ about the interface, and by keeping up to quadratic terms it is possible to map this problem to that of a Brownian particle subject to a parabolic potential of the form

$$V(z') = \frac{\gamma^2}{2} z'^2 \quad (7)$$

This first approximation is similar to the potential for linear elasticity. For a step function as the initial condition, of width 2δ and height P_0 , the solution of eq 5 with $V(z')$ given by eq 7 is¹¹

$$P(z', t) = \frac{\delta P_0 e^{\gamma t}}{2} \left(-\operatorname{erf} \left[\frac{z' - \delta e^{-\gamma t}}{2\sqrt{\left(\frac{D}{2\gamma}(1 - e^{-2\gamma t})\right)}} \right] + \operatorname{erf} \left[\frac{z' + \delta e^{-\gamma t}}{2\sqrt{\left(\frac{D}{2\gamma}(1 - e^{-2\gamma t})\right)}} \right] \right) \quad (8)$$

From this local expression of $P(z', t)$ in the vicinity of the interface ($z' \approx 0$) one can reasonably propose as an Ansatz that the width ω in eq 4 may be approximated by

$$\omega(t) = 2\sqrt{\left(\frac{D}{2\gamma}(1 - e^{-2\gamma t})\right)} \quad (9)$$

It should be noted that eq 8, for short times, is the solution to Fick's second law, and most importantly, eq

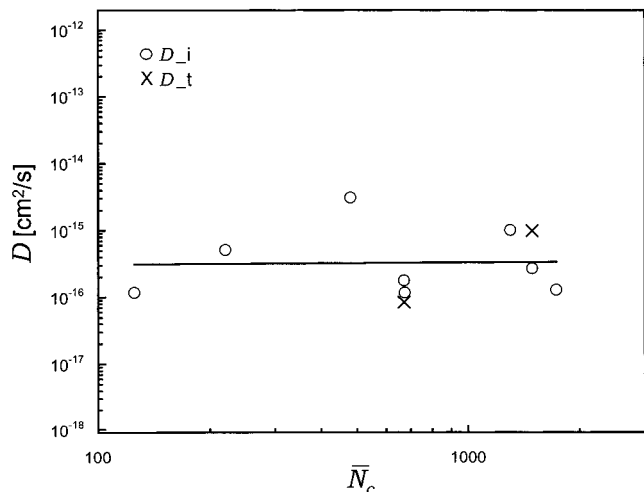


Figure 4. Diffusion constants as a function of \bar{N}_c .

9 is consistent with the long time behavior which is observed experimentally. Figure 3 shows the fits of eq 9 (continuous curves) to the network–network interfacial widths, as a function of time, for samples with $\bar{N}_c = 140$ and $\bar{N}_c = 1510$. The time variable, t , in the fits of eq 9 was taken to be of the form $t \rightarrow t + t_0$, which accounts for an initial roughness of the interface by allowing the initial width at $t = 0$ be different from zero. In fitting the neutron reflectivity profiles, the roughness of the polymer–air and polymer–Si interfaces was included as fitting parameters. The roughness of these interfaces remained equal to each other and essentially independent of time and equal to or less than about 10 Å. This is also consistent with X-ray reflectivity measurements made on the polymer films prior to bilayer formation, which gave an initial polymer–air roughness of about 10 Å or less. The air–polymer and the polymer–Si interfaces show no evidence of cross-link density dependent roughness. As representative of these interfaces, the value of the polymer–air roughness for both samples is plotted in Figure 3. The changes observed in the reflectivity profiles is due to a systematic increase in the (hydrogenated) polymer/(deuterated) polymer interfacial width. Figure 4 shows the values obtained for D , the effective diffusion coefficient, as a function of \bar{N}_c for all samples. From the figure it is clear that D is approximately constant as a function of \bar{N}_c with the values of D between 1 and 3 orders of magnitude smaller than those found for linear polymers diffusing into networks.⁵ Since the networks cannot undergo long-range interdiffusion, it is not clear that D should depend on \bar{N}_c . To establish any dependence of D on \bar{N}_c , very precise measurements of the interfacial width at short annealing times, prior to the width reaching its equilibrium value, would need to be made.

Figure 5 shows the values obtained for $w(t \rightarrow \infty)$ or equilibrium widths, w_{eq} , as a function of \bar{N}_c for all the samples. The equilibrium interfacial widths are found to be of the order of Rg_c , the radius of gyration of the network mesh, consistent with those found by Geoghegan et al.¹⁰ The continuous line in Figure 5 corresponds to a fit to the equilibrium widths of the form \bar{N}_c^α , with $\alpha = 0.47 \pm 0.1$, which complements the work by Geoghegan et al. where no clear relation between w_{eq} and \bar{N}_c was established. It is found that the uncertainty in the values of \bar{N}_c has no effect on the value of α . The error bars in the values of \bar{N}_c , which, for clarity, are not included in the figure, are about the size of their

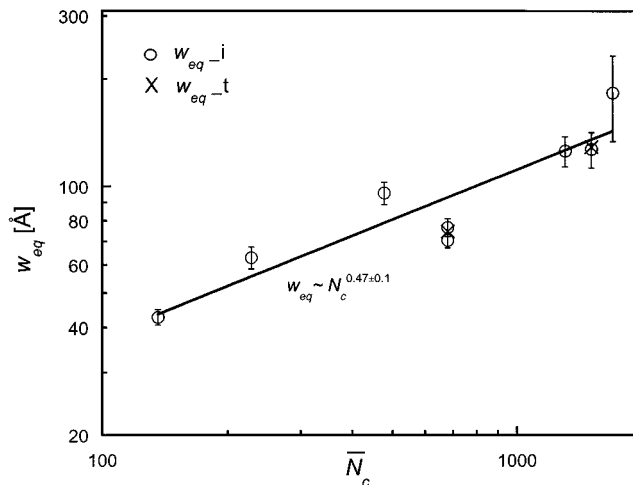


Figure 5. Equilibrium widths, w_{eq} , as a function of \bar{N}_c . The solid line represents a fit of the form $w_{eq} \sim \bar{N}_c^\alpha$, where α is found to be 0.47 ± 0.1 .

corresponding symbol, except for the sample with $\bar{N}_c = 1700$ where the error bar is only slightly larger than the symbol. The uncertainty in the measurement of the exponent of \bar{N}_c comes from sample preparation differences as can be seen in samples with $\bar{N}_c = 680$ and to the uncertainty in the fits to the reflectivity data.

The broadening of the interfacial width is caused by local chain rearrangements, which are driven by the local free energy. At a scale comparable to Rg_c , both the dangling ends and chains between cross-links in the vicinity of the interface can in principle broaden the interface. For the chains between cross-links, interdigitation comes at the expense of significant conformational entropy and probably contributes little to interfacial broadening, whereas the dangling ends, free at one end, can redistribute at the interface and thus broaden the interfacial width.²⁸ Interdigitation of the dangling ends causes no interfacial swelling of one film due to the other because the interface is symmetrical, and we can ignore swelling effects. Asymmetry can arise if the interface is very close to the Si wall (at a distance of the order of $2Rg_c$).²⁷ The physical model of the network–network interface in this scenario corresponds to that of a brush (the dangling ends) in contact with an athermal polymer melt (the network). The state diagram for a brush in contact with a polymer melt, presented by Ferreira et al., shows the different brush conformations as a function of the brush surface density and the brush and the polymer melt weight-average chain lengths.^{29–33} For the purpose of investigating scaling trends, the dangling ends of the network and the network mesh have a weight-average chain length proportional to \bar{N}_c , and a simple estimate of Σ , the interfacial dangling end density, gives a $\bar{N}^{-1/2}$ dependence, where \bar{N} is the weight-average chain length of the original polymer prior to cross-linking. This places the system studied in the screened wet brush region of the state diagram. The screened wet brush region is where an overlapping brush has an ideal conformation due to screening by the surrounding chains from the melt. This means that the height of the brush scales as $\bar{N}_c^{1/2}$. Since the interface equilibrium width, w_{eq} , is equivalent to the brush height, this scaling behavior agrees with what is observed experimentally.

Because the network is random at scales much larger than Rg_c , there can be significant fluctuations in cross-

link density throughout the network. Using γ -ray cross-linking leads to a statistically random location of cross-link junctions due to the large penetration depth for γ -rays. This is in contrast to some chemically cross-linked systems where significant clustering of the cross-link junctions can occur due to chemical reaction kinetics.³⁴ The lower cross-link density areas form soft regions which can cause the interface to broaden, and Geoghegan et al. noticed that this rearrangement process is driven by the free energy for a blend of networks at the interface. Using the expressions obtained by Broseta et al. in the calculation of the interfacial width between two homopolymers of finite size, Geoghegan et al. calculated the expected scaling behavior of the interfacial width between two networks as a function of the cross-link density and found that the interfacial broadening also scaled as $\bar{N}_c^{1/2}$.^{10,35} It is unclear whether these soft regions are able to form entanglements. A locally sharp interface would be inconsistent with the results found on interfacial adhesion experiments on equivalent systems, where the adhesion energy was found to depend on the cross-link density of the networks.³⁶ However, both effects, the dangling ends and the soft regions broadening the interface, can act simultaneously, in an adding fashion, leaving the overall scaling behavior unaffected.

The interfacial broadening behavior between bilayers formed with independently cross-linked films and bilayers formed with un-cross-linked films which then were cross-linked as a unit were observed to be equivalent (Figure 3). The interfacial equilibrium widths and diffusion constants for these two types of bilayers were equal within experimental error (Figures 4 and 5), and hence, the interdiffusion behavior in these systems is not affected by the two different methods of forming the bilayers.

Conclusions

It is found that the kinetics of network–network interfacial broadening is accurately described by an analysis using the Fokker–Planck equation with an external potential. The measured equilibrium interfacial widths scale with \bar{N}_c with an exponent of 0.47 ± 0.1 . The models that best describe this system are, at a scale of order Rg_c , a brush in contact with a polymer melt and, at a scale of several Rg_c , interfacial rearrangements driven by the interfacial free energy of a network–network blend. The scaling behavior of the equilibrium interfacial width, as a function of \bar{N}_c , is predicted to be, in both models, $\bar{N}_c^{1/2}$, which is observed experimentally. The values of the equilibrium interfacial widths are on the order of the radius of gyration of the network mesh. The diffusion constant, D , was found to be independent of \bar{N}_c within the accuracy of the experiment. Since the network cannot undergo long-range interdiffusion, it is not clear the D should depend on \bar{N}_c . The two types of cross-linked film bilayers used in this study, bilayers formed with independently cross-linked films and bilayers formed before being cross-linked, gave equivalent results for interfacial broadening behavior, equilibrium widths, and diffusion constants.

Acknowledgment. The authors thank Emeritus Professor Joseph Silverman, whose suggestions made the preparation of cross-linked polystyrene films possible. We also thank Mr. Vincent Adams, Associate Director of Radiation Facilities in the Department of

Materials and Nuclear Engineering, University of Maryland, for his help in the vacuum γ irradiation of the samples, performed in this facility. Dr. Lipin Sung and Dr. Robert Ivkov of the National Institute of Standards and Technology are acknowledged for their help in data collection and reduction at the NG7 reflectometer at the NIST Center for Neutron Research. Finally, U. Perez-Salas also thanks CONACYT (Consejo Nacional de Ciencia y Tecnología) for its support of this work.

References and Notes

- (1) Composto, R. J.; Kramer, E. J. *Macromolecules* **1988**, *21*, 2580.
- (2) Jordan, E. A.; Ball, R. C.; Donald, A. M.; Fetters, L. J.; Jones, R. J. *Macromolecules* **1988**, *21*, 235.
- (3) Antonietti, M.; Sillescu, H. *Macromolecules* **1985**, *18*, 1162.
- (4) Gent, A. N.; Kaang, S. Y. *J. Polym. Sci., Polym. Phys. Ed.* **1989**, *27*, 893.
- (5) Zheng, X.; Rafailovich, M. H.; Sokolov, J.; Zhao, X.; Briber, R. M.; Schwarz, S. A. *Macromolecules* **1993**, *26*, 6431.
- (6) de Gennes, P. G. *J. Chem. Phys.* **1971**, *55*, 572.
- (7) Briber, R. M.; Bauer, B. J. *Macromolecules* **1991**, *24*, 1899.
- (8) Briber, R. M.; Liu, X.; Bauer, B. J. *Science* **1995**, *268*, 395.
- (9) Flory, P. J. *Principles of Polymer Chemistry*; Cornell University Press: Ithaca, NY, 1953.
- (10) Geoghegan, M.; Boue, F.; Bacri, G.; Menelle, A.; Bucknall, D. G. *Eur. Phys. J. B* **1998**, *3*, 83.
- (11) Risken, H. *The Fokker–Planck Equation: Methods of Solution and Applications*, 2nd ed.; Springer Series in Synergetics; Springer-Verlag: Berlin, 1989; Vol. 18.
- (12) *Handbook for Radiation Chemistry of Polymers*, 3rd ed.; John Wiley: New York, 1980.
- (13) Charlesby, A. *Atomic Radiation and Polymers*; Pergamon Press: New York, 1960.
- (14) Parkinson, W.; Keyser, R. *Radiation Chemistry of Macromolecules*; Academic Press: New York, 1973; Vol. II.
- (15) Mark, J. E., Ed.; *Physical Properties of Polymers Handbook*; AIP Press: Woodbury, NY, 1996.
- (16) Patel, S. K.; Malone, S.; Cohen, C.; Gillmor, J. R.; Colby, R. H. *Macromolecules* **1992**, *25*, 5241.
- (17) Anker, J. F.; Majkrzak, C. F.; Satija, S. K. *J. Res. NIST* **1993**, *98*, 47.
- (18) Hamilton, W. A.; Hayter, J. B.; Smith, G. S. *J. Neutron Res.* **1994**, *2*, 1.
- (19) Yethiraj, M.; Fernandez-Baca, J. A. *Neutron Scattering Mater. Sci. II* **1995**, 59.
- (20) Mirror/Interface Reflectivity Rig (Oak Ridge). Operation shell and acronym: Hayter, J. B. (1989–1993). Instrument control, data collection, reduction, and analysis routines: Hamilton, W. A. (1991–1998). Neutron Scattering Section, Solid State Division, Oak Ridge National Laboratory. During this work Oak Ridge National Laboratory has been managed for the U.S. Department of Energy by Lockheed Martin Energy Research Corporation under Contract DE-AC05-96OR22464 and by UT-Batelle LLC under Contract DE-AC05-00OR22725.
- (21) Russell, T. P. *Mater. Sci. Rep.* **1990**, *5*, 171.
- (22) Crank, J. *The Mathematics of Diffusion*, 2nd ed.; Oxford University Press: Oxford, UK, 1975.
- (23) Karim, A.; Mansour, A.; Felcher, G. P. *Phys. Rev. B* **1990**, *42*, 6846.
- (24) Karim, A.; Felcher, G. P.; Russell, T. P. *Macromolecules* **1994**, *27*, 6973.
- (25) Gennes, P. G. D. *Soft Interfaces. The 1994 Dirac Memorial Lecture*, 2nd ed.; Cambridge University Press: New York, 1997.
- (26) Smith, G. S.; Hamilton, W. A.; Fitzsimmons, M.; Baker, S. M.; Hubbard, K. M.; Nastasi, M.; Hirvonen, J.-P.; Zocco, T. G. *SPIE* **1992**, *1738*, 246.
- (27) Zheng, X.; Sauer, B. B.; Alsten, J. G. V.; Schwarz, S. A.; Rafailovich, M. H.; Rubinstein, J. S. M. H. *Phys. Rev. Lett.* **1995**, *74*, 407.
- (28) Brochard-Wyart, F.; de Gennes, P. G.; Leger, L.; Marciano, Y.; Raphael, E. *J. Phys. Chem.* **1994**, *98*, 9405.
- (29) de Gennes, P. G. *Macromolecules* **1980**, *13*, 1069.
- (30) Brochard, F. *J. Phys. (Paris)* **1981**, *42*, 505.
- (31) Wijmans, C.; Zhulina, E.; Fleer, G. *Macromolecules* **1994**, *27*, 3238.
- (32) Gay, C. *Macromolecules* **1997**, *30*, 5939.

- (33) Ferreira, P. G.; Ajdari, A.; Leibler, L. *Macromolecules* **1998**, *31*, 3994.
- (34) Bastide, J.; Leibler, L.; Prost, J. *Macromolecules* **1990**, *23*, 1821.
- (35) Broseta, D.; Fredrickson, G. H.; Helfand, E.; Leibler, L. *Macromolecules* **1990**, *23*, 132.
- (36) Perez-Salas, U. Polystyrene Network-Network Interfaces: Adhesion and Interdiffusion. Ph.D. Thesis, University of Maryland, 2000.

MA010842Y